



Data report: coring disturbances in advanced piston cores from IODP Expedition 398, Hellenic Arc Volcanic Field¹

Contents

- 1 Abstract
- 1 Introduction
- 2 Methods
- 2 Results
- 10 Summary
- 11 Acknowledgments
- 11 References

Keywords

International Ocean Discovery Program, IODP, JOIDES Resolution, Expedition 398, Hellenic Arc Volcanic Field, coring disturbance, volcanoclastic, sediment, core, drilling, flow-in

Supplementary material

References (RIS)

MS 398-203

Received 8 August 2024
Accepted 27 January 2025
Published 25 April 2025

Martin Jutzeler,² Acacia S. Clark,³ Michael Manga,³ Iona McIntosh,³ Tim Druitt,³ Steffen Kutterolf,³ and Thomas A. Ronge³

¹ Jutzeler, M., Clark, A.S., Manga, M., McIntosh, I., Druitt, T., Kutterolf, S., and Ronge, T.A., 2025. Data report: coring disturbances in advanced piston cores from IODP Expedition 398, Hellenic Arc Volcanic Field. In Druitt, T.H., Kutterolf, S., Ronge, T.A., and the Expedition 398 Scientists, Hellenic Arc Volcanic Field. *Proceedings of the International Ocean Discovery Program*, 398: College Station, TX (International Ocean Discovery Program). <https://doi.org/10.14379/iodp.proc.398.203.2025>

² Centre for Ore Deposit and Earth Sciences, School of Natural Sciences, University of Tasmania, Australia. Correspondence author: jutzeler@gmail.com

³ Expedition 398 Scientists' affiliations.

Abstract

Coring disturbances can affect the properties and interpretations of advanced piston cores collected during International Ocean Discovery Program (IODP) expeditions. IODP Expedition 398 in the Hellenic arc, Greece, used piston cores for unconsolidated and commonly thick volcanoclastic successions ranging from fine ash to lapilli intervals that are interbedded with cohesive carbonate oozes. The occurrence of thick intervals of loose, low-density clasts (pumice) and ash made coring operations difficult. Several instances of partial strokes were recorded by the drilling data, and flow-in coring disturbances occur over multiple cores, particularly where the volcanoclastic sediment is not confined by carbonate oozes. Moreover, strong rheological contrast between intervals favored midcore flow-in and, to a lesser extent, liquefaction and shearing. Collapse of the borehole enabled coring of fall-in that was recovered at the top of some cores. In addition, some cores experienced further disturbances during horizontal storage after recovery, affecting physical properties. These various disturbances in piston cores are important to identify because they affect the nature of the core, mix multiple strata, modify stratigraphy, and affect the shipboard analyses of physical properties and hence how geophysical data are interpreted. Visual identification of the coring disturbances presented in this report is based on core photographs that were reviewed by a single person over a few days to ensure uniformity in data acquisition. This report was produced to inform and guide current and future interpretations of data from these cores, which can affect stratigraphy and hence the reconstruction of eruption chronology, deposit thickness, and emplacement mechanisms.

1. Introduction

From 11 December 2022 to 10 February 2023, International Ocean Discovery Program (IODP) Expedition 398 drilled and cored volcanic successions in the Hellenic arc, Greece (Druitt et al., 2024a). Cores from the drill sites are chiefly composed of volcanoclastic intervals interpreted by shipboard scientists to record submarine and subaerial volcanism from the Miocene to present interbedded with carbonate ooze. Drilling in volcanic environments is known to be technically difficult (Jutzeler et al., 2014) owing to poor borehole stability in loose and coarse granular sediment, as well as the physical properties of the volcanoclastic sediment (e.g., Newtonian fluid behavior). Furthermore, recovery of pristine cores of unconsolidated material by advanced piston corer (APC) coring is challenging because the piston may not fully deploy in either the coarse or the Newtonian fluid-like material (well-sorted silt, sand, and/or pebbles) and recovery of sediment with high intergranular porosity makes it prone to sustained fluid flow and liquefaction (Jutzeler et

al., 2014). The coring disturbances form through liquefaction, movement, and loss and/or addition of sediment in the core, and they vary in severity, location, and extent depending on the coring conditions and the material encountered (Jutzeler et al., 2014).

The lithologies cored during Expedition 398 include very thick beds of granular volcanoclastic material interbedded with cohesive carbonate oozes; the former includes low-density pumice lapilli (>2 mm) that are prone to entrainment by water motion. The shipboard party documented coring disturbances while logging cores (Kutterolf et al., 2024; Druitt et al., 2024a) and produced illustrations of identified coring disturbances in each site chapter (Druitt et al., 2024a) and the methods chapter (Kutterolf et al., 2024). With two shifts of scientists and an evolving understanding over the 2 month cruise period, however, significant coring disturbances may have been missed. Postexpedition in-depth analyses of core photographs and core descriptions enabled us to identify multiple intervals of core disturbance in addition to the disturbances described on board (Druitt et al., 2024b). For example, basal flow-in and midcore flow-in disturbances can be difficult to identify, and we suggest here that several were not identified on the ship. A particular difficulty resides in being able to visualize multiple sections and cores together to fully identify the extent of these disturbances. This is especially challenging shipboard because core descriptions are commonly done section by section. This paper is based on a holistic postexpedition assessment of the coring disturbances based on the core photographs in an effort to limit biases. The shipboard list of brecciated core disturbances is not documented in this study because they can be readily identified from photographs. Furthermore, we focused on APC cores only (H = APC and F = half-length APC [HLAPC] barrels), whereas the shipboard data extend to all core types. Our list is otherwise intended to be a more comprehensive assessment and supersedes the shipboard data for all APC cores (Table T1; see COREDATA in [Supplementary material](#)).

During Expedition 398, a substantial number of APC cores (H and F cores) experienced coring disturbance that affected the integrity of the various volcanoclastic and carbonate ooze intervals; these were recorded visually (Druitt et al., 2024a) but are also discernible through physical properties such as magnetic susceptibility (MS), bulk density, and seismic velocity. The coring disturbances present in Expedition 398 cores are similar to those identified during Integrated Ocean Drilling Program Expedition 340 in the Lesser Antilles arc (Expedition 340 Scientists, 2013; Le Friant et al., 2015; Jutzeler et al., 2014, 2016), IODP Expedition 350 at Site U1436 in the Izu-Bonin-Mariana arc (Tamura et al., 2015), and Ocean Drilling Program (ODP) Leg 126 in the Izu-Bonin arc region (Taylor, Fujioka, et al., 1990; Jutzeler and White, 2013). Similar to Jutzeler et al. (2016), this data report provides a comprehensive list of the various types of coring disturbances identified in all advanced piston cores recovered during the expedition. Furthermore, it provides visual descriptions and physical property data sets that demonstrate the nature and extent of these disturbances.

2. Methods

Coring disturbances in H and F cores (APC coring exclusively) were visually identified and classified postexpedition by a single person (M. Jutzeler) over a short period (<1 week) to improve consistency in data acquisition. Identification was carried out from medium-resolution core composite photographs, and high-resolution core photographs were used for challenging intervals. The use of composite core photographs provides the vertical context in the sedimentary succession that can be difficult to ascertain while on the ship, allowing for in-depth analysis of the integrity of the cores. Fall-in and basal flow-in were also compared to their potential lithologic sources in the core immediately above and below, respectively. Physical properties such as bulk density and seismic velocity were not systematically used, but MS helped to identify the extent of some basal flow-in disturbances. These observations are based on, and complement, earlier studies (Jutzeler et al., 2014, 2016).

3. Results

All coring disturbances are listed in Table T1, and additional comments and data are available in COREDATA in [Supplementary material](#). The disturbances are organized per core and per dis-

Table T1. Coring disturbances in APC and HLAPC cores, Expedition 398. [Download table in CSV format.](#)

turbance type, and one of two levels of confidence (confident versus possible) is proposed for each occurrence. Data in Table T1 and COREDATA in **Supplementary material** supersede disturbance in APC cores depicted in the visual core descriptions (VCDs) produced by the shipboard party (Kutterolf et al., 2024; Druitt et al., 2024a). Brecciated core described in the VCDs and the drilling disturbances in extended core barrel (XCB) and rotary core barrel (RCB) cores are not assessed here.

Of the 477 APC cores (F and H barrels) collected during Expedition 398 and examined in this study, 240 (50.3%) were confidently judged as disturbed or judged to possibly have been affected by coring disturbances. Fall-in occurs in 21.6% (possibly up to 30.1%) of the cores, whereas basal flow-in is present in 64.1% (possibly up to 73.4%) of the cores. A further 8.9% of the cores have midcore flow-in. Extension, liquefaction, and shearing occur in 12.4% of the cores. Importantly, although these statistics may seem high, these percentages are per core and thus not representative of core length, which brings a much lower percentage. Most cores are only affected over a few meters each, and thus most of the cored intervals hold pristine sedimentary records.

The distinguishing features for each disturbance type are described below, followed by specific Expedition 398 observations.

3.1. Fall-in

Fall-in disturbance represents collapsed material that accumulates at the bottom of the borehole and is accidentally sampled in the uppermost part of the next piston core (Jutzeler et al., 2014). Fall-in is commonly a few tens of centimeters thick but can extend to more than 1 m and can consist of clast-supported, graded or ungraded, lapilli-sized material; a slurry of carbonate ooze and lapilli; or rare carbonate ooze fragments (Jutzeler et al., 2014) (Figure F1). Fall-in intervals are likely to be of polymict componentry because they consist of material from various intervals above

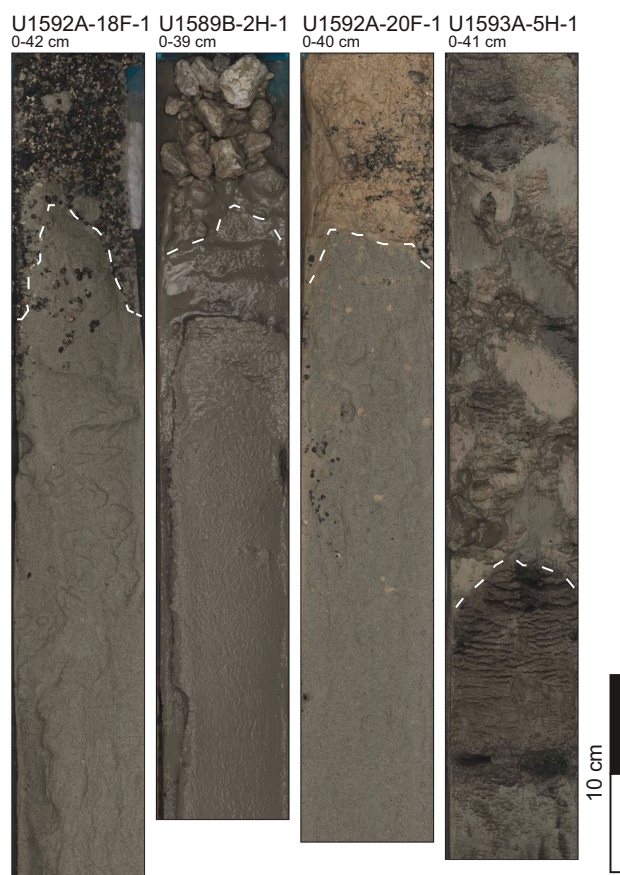


Figure F1. Examples of cores affected by fall-in, Sites U1589, U1592, and U1593. Collapsed material from the borehole is sampled at the top of the next core, resulting in clast- or matrix-supported, coarse- or fine-grained material that extends from a few centimeters to tens of centimeters from the top of the core. Dashed lines = lower boundary of fall-in interval.

in the borehole. The fall-in material is theoretically derived from anywhere in the borehole above, although it is more likely to comprise material from the core immediately above. Although fall-in is relatively easy to identify, it is important to check the nature of the core immediately above and assess whether the interpreted fall-in could be a natural continuation of a sedimentary breccia interval that straddles the two cores.

The occurrence of fall-in in Expedition 398 cores follows the general observations, and fall-in intervals are commonly obvious due to the occurrence of an abnormal breccia that is difficult to reconcile with the overall succession. A few examples are uncertain because of the relatively coarse grain size in adjacent intervals.

3.2. Basal flow-in

Basal flow-in is the most destructive coring disturbance because it corresponds to intake of borehole material from the bottom of the core barrel (i.e., the cutting shoe) while the piston completes its deployment during recovery (Jutzeler et al., 2014). The common cause of basal flow-in is the resistance of granular material (e.g., sand and gravel, or ash and lapilli) to coring, which prevents the full deployment of the piston, resulting in a partial stroke. This results in partial to complete liquefaction of the loose sediment at the bottom of the core and potential loss of material through the core catcher. Another cause may be associated with the inability of the core catcher to seal the bottom of the hole during recovery. Basal flow-in creates loose, soupy, commonly normally graded sand-sized material at the base of the core that can be extensive over several meters from the base of the core and, in some extreme cases, up to its top (Jutzeler et al., 2014). It remains difficult to evaluate what proportion of material was removed or added to the core during retrieval (Jutzeler et al., 2014); however, recovery of soupy sediment may attest to severe coring-based liquefaction. Whole-round MS has very smooth trends and overall increases downcore, recording density sorting in the liquefied sediment during core recovery, with dense, magnetic ferromagnesian minerals preferentially settling at the base of the core and poorly magnetic, felsic ash at the top (Jutzeler et al. 2014). Variations in point-analysis MS (MSP) (measured on the top surface of the split core) record heterogeneities in the liquefied sediment and/or postsplitting lateral movement and settling of sediment slurries in the core section (see **Shipboard disturbances**). These values also vary from core section to core section, depending on the orientation of the core during transport by the crew and while laid on deck upon splitting (Jutzeler et al., 2014). Seismic *P*-wave velocity becomes homogeneous and slightly increases downcore, also reflecting density sorting by settling within the core during recovery. Bulk density (measured using gamma ray attenuation [GRA]) trends are much smoother than in undisturbed sediment and record overall increasing trends downcore, although large steps in values occur at core section boundaries. Peaks and troughs in values of density are correlated with the volume present in the analyzed interval; cores that experienced basal flow-in can be half empty (Jutzeler et al., 2014), and measured densities can be less than seawater.

In Expedition 398 cores, several cases of repeated basal flow-in over several cores following partial strokes occur throughout coarse-grained pumiceous deposits, with an extreme example in Hole U1592A (Table **T1**). The combined analysis of coring disturbances using core photographs and physical properties provides further understanding of the extent of disturbances in Expedition 398 cores (Figures **F2**, **F3**). Sediment grading along the length of the split core surface indicates settling of liquefied sediment while the core was resting horizontally (green arrows in Figure **F2**), and physical property data sets may exhibit sharp breaks in overall downcore trends at section boundaries (Figure **F3**), matching textures described in Jutzeler et al. (2014).

Figure F2 (facing page). Examples of cores from Holes U1590A, U1591A, and U1593 affected by intense basal flow-in. Yellow arrows = interpreted boundaries between undisturbed stratigraphy (above) and sediment affected by basal flow-in (below); green arrows = grading along the length of the core, exemplifying liquefied sediment settling while the core was resting horizontally on the ship (Jutzeler et al., 2014). In Core 398-U1590A-4H, homogeneous sediment has a soupy texture. Blue arrow = sediment disintegration and injection of ash (sand) between more cohesive lithologies (similar to midcore flow-in). In Core 398-U1591A-3H, liquefied sediment was density graded while in a vertical position, demonstrated by the dark-to-light-colored gradient upsection from the core catcher to Section 3H-4. The dark-light grading corresponds to upcore change from denser, low-vesicularity volcanic clasts and ferromagnesian minerals to less dense, high-vesicularity pumice and vitric ash components. This density grading is noticeable in MS data (see Figure F3), as well (Jutzeler et al., 2014). In Core 398-U1593B-29F, the core is entirely disturbed, showing excellent normal grading resulting from vertical settling in a liquefied slurry during recovery. Partial deployment of the piston in the lithology noted by the drillers (i.e., partial stroke; see drilling reports) resulted in poor recovery and basal flow-in disturbance (Jutzeler et al., 2014). (Figure shown on next page.)



3.3. Midcore flow-in

Midcore flow-in can occur anywhere in the core (Figure F4) and represents the vertical migration of an initially well-sorted ash (or silt or sand) interval that forms a slurry and is rapidly injected into a cavity within a more cohesive interval, typically carbonate ooze (Jutzeler et al., 2014). The cavity is formed by intense vertical stretching within the core liner in response to the extensional stress exerted on the core as it is recovered and then retrieved to the surface via wireline. The midcore flow-in ash should be identical in composition to an ash interval above or below the stratigraphy in which it is found, although some mixing with material from nearby layers may occur. The original ash layer would be strongly liquefied and show evidence of sediment depletion. Fur-

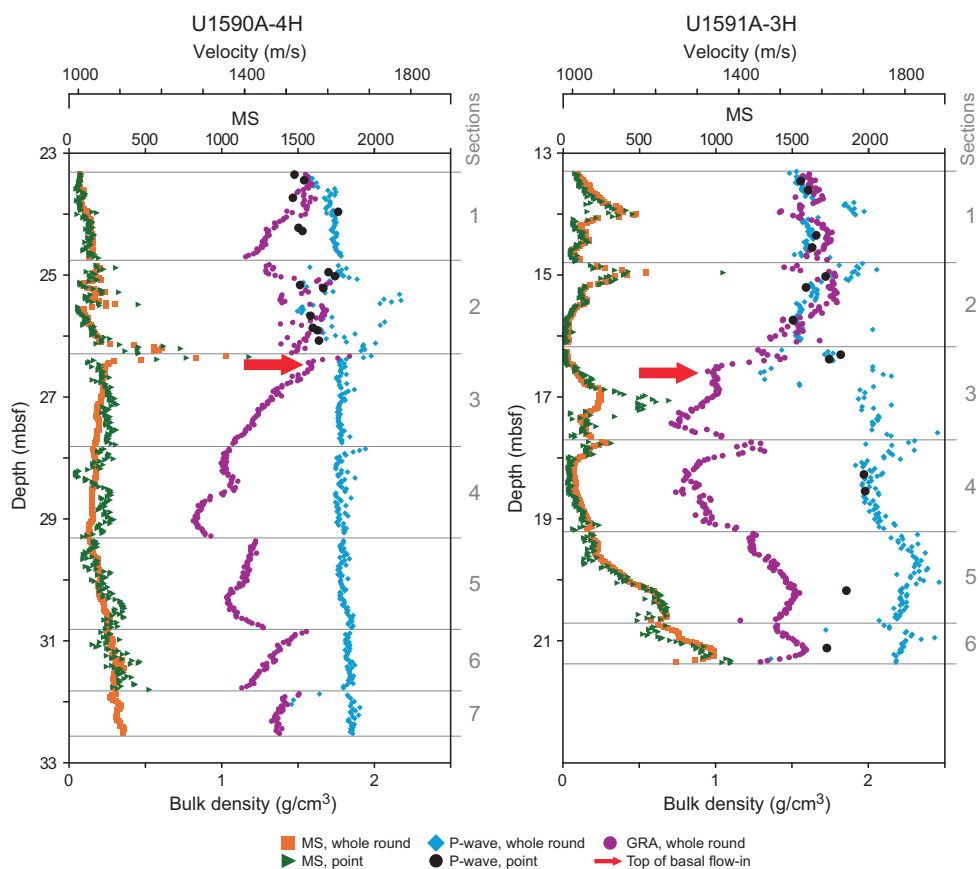


Figure F3. MS (IU), GRA bulk density, and *P*-wave velocity for two cores that experienced strong basal flow-in (Figure F2; note section numbers on right for comparison). All physical properties show strong variations at the onset of the basal flow-in (red arrow). In Core 398-U1590A-4H, the positive spike in MS corresponds to the last undisturbed unit, which is a very dark ash layer rich in ferromagnesian minerals. The sudden drop in MS clearly demonstrates that the basal flow-in replaces this stratigraphy with material that is less magnetic. The whole-round MS increases downcore, exemplifying density sorting of a well-mixed, liquefied material during core recovery. MSP measurements from the top surface of the split core follow the whole-round MS trend but show greater disparities, including sinusoidal variations, within the disturbed sediment that are averaged out in the whole-round data by the larger sensitivity window on the WRMSL sensor. These disparities demonstrate the core material was water saturated and liquefied, enabling density settling of sediment to occur while the core sections were stored in a horizontal position prior to splitting. The bulk density data also showcase complex behavior occurring after the division into core sections, with extreme steps in values at core section boundaries, yet shows a general drop in density within the disturbed material with density settling during core recovery reflected in a downcore increase in section-average density values. The sediment velocity increases downcore reflecting the density settling during core recovery. The velocity values are very homogeneous in the disturbed section in contrast to most of the undisturbed stratigraphy. Core 398-U1591A-3H shows similar characteristics, with a very strong gradient in MS downcore in the disturbed sediment that matches the color change in the core due to an increase in dark, magnetic minerals (i.e., ferromagnesian minerals) at the base of the disturbed core (Figure F2). The bulk density shows minor steplike behavior at core section boundaries, and values overall increase downcore within the disturbed material. The positive peak in bulk density (and in velocity and MS to a minor extent) at the boundary between Sections 3H-3 and 3H-4 is bounded by two troughs; these values are proportional to the volume of sediment present along the core (Figure F2). Velocities have larger variations than in Core 398-U1590A-4H and are partly associated with core section boundaries.

ther, a smear of ash may occur along the core liner, identifying sediment flowage (Jutzeler et al., 2014), although this can be very faint and/or not appear on the core split surface. Allowing a 3D view of the core, tomography may help resolve such uncertainties in sediment flowage.

Midcore flow-in can be difficult to identify because it may look similar to primary ash layers and can also resemble slump or debris flow deposits. The disturbance can be recognized by floating artificial clasts of carbonate ooze within ash, irregular but sharp contacts between ash and carbonate ooze intervals, and excellent continuity in textures (sometimes jigsaw fit) in the carbonate ooze intervals on both sides of the volcanoclastic layer (Figure F4). Boudinage trains of carbonate ooze separated by uniform granular material is also possible.

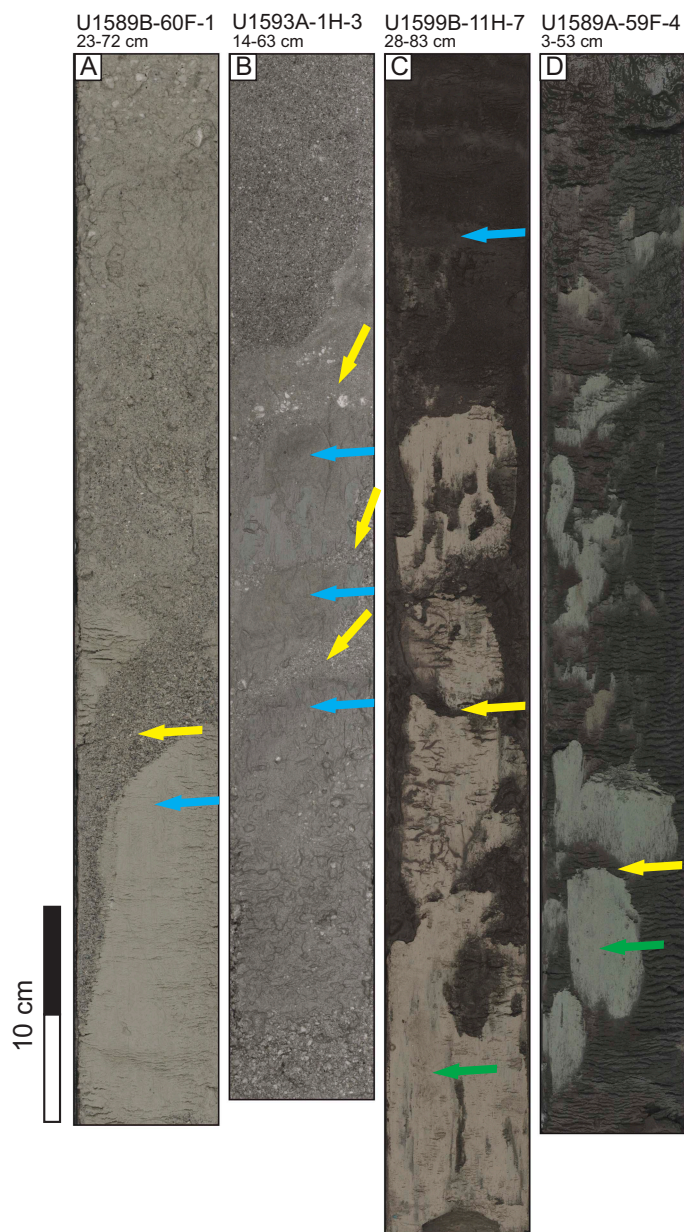


Figure F4. Examples of cores affected by midcore flow-in, Sites U1589, U1599, and U1593. A. Injection of coarse ash (yellow arrow) in tuffaceous mud (blue arrow); the ash is similar to an interval of liquefied ash immediately below. B. Multiple injections of ash and pumice pebbles (yellow arrows) in between undisturbed finer ash (blue arrow), resembling multiple natural sediment intervals. C, D. Multiple injections of fine black ash (yellow arrows) inside carbonate ooze (green arrow), and shearing of the carbonate ooze (middle right). Undisturbed dark sediment (blue arrow) rests immediately above the disturbed black ash.

Examples of midcore flow-in within Expedition 398 cores are pictured in Figure F4. Interestingly, there is no clear correlation between the pulling force recorded by the drillers and the presence of midcore flow-in disturbances in these cores (Figure F5; see COREDATA in [Supplementary material](#)), strongly suggesting that the local rheological contrast between formations is the main control on such sediment migration. This suggests that midcore flow-in disturbances may occur from vertical stress in the core during travel up to the drilling platform as well as during initial recovery from the formation. Midcore flow-in was also recorded at Site U1436 during IODP Expedition 350 (Tamura et al., 2015).

3.4. Extension, liquefaction, and shearing

Stretching of the core during separation from the formation, tumbling in the drill pipe during recovery, rotation, and transfer into a horizontal position can all contribute to affecting the integrity of the core (Jutzeler et al., 2014). Through these processes, granular intervals can suffer from extension, liquefaction, and/or shearing, resulting in partial to complete loss of stratification (Jutzeler et al., 2014).

In Expedition 398 cores, these disturbances remain minor, and if bound by stiffer layers, the integrity of each stratigraphic layer is commonly preserved (Figure F6). Carbonate ooze may also be sheared, especially at the bottom of the core.

3.5. Shipboard disturbances

The cores affected by basal flow-in commonly exhibit soupy sediment in partially filled core liners while they are stored horizontally prior to splitting. Settling of the sediment before being split results in density grading along the length of the core liner (Jutzeler et al., 2014), as described in [Basal flow-in](#).

In the case of severe basal flow-in during Expedition 398, the sediment was manually compacted within the core liner using a plunger on the core deck (Table T1) prior to sectioning the cores; such action likely results in stratigraphic disruption. Less commonly, some core liners shattered while on the catwalk due to sediment overpressure, and core technicians had to extrude the core to a new liner (Table T1), potentially disrupting sediment stratigraphy and associated physical properties. Additional cryptic disturbance was possible during laboratory processing of the cores. A previously unreported onboard experiment was undertaken on a typical core section (398-U1599B-27F-2) containing pumice lapilli to assess possible cryptic disturbances to granular sediment physical properties while waiting for the core to be measured and split. The chosen section is composed of coarse pumice lapilli and ash that appeared to the shipboard scientists to have been

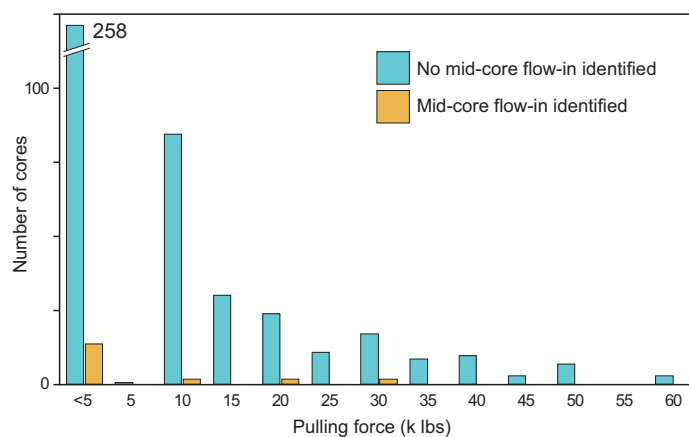


Figure F5. Midcore flow-in plotted against pulling pressure (in thousands of pounds) during recovery from the bottom of the borehole, Expedition 398. No statistical correlation could be demonstrated, suggesting that the rheological variations between units of different lithology is the dominant cause of sediment flow, as postulated by others (McCoy et al., 1985; Jutzeler et al., 2014). This also suggests that midcore flow-in may result from vertical core extension by sagging under its own weight during ascent to the drilling deck.

liquefied into a water-saturated slurry, and thus it was a possible candidate for basal flow-in (Figure F7; Table T1), although it does not show the obvious signs of sediment redistribution in the form of an along-section gradient in density. After being cut into 1.5 m long whole-round core sections, the sections are stored on horizontal racks for at least 2 h to equilibrate to room temperature. Depending on core recovery and backlog, a core section may be stored for >10 h before its physical properties are measured. The Whole-Round Multisensor Logger (WRMSL) mechanically moves the core section in a channel where it analyzes MS, *P*-wave velocity, and GRA bulk density with a sampling interval of 2.5 cm. Details of the instruments are provided in Kutterolf et al. (2024). To investigate the disturbances that may occur during horizontal storage on deck, the chosen section was passed through the WRMSL three times: 10 min after the core was recovered on the catwalk and then twice 14 h later, with the two repeat measurements separated by 9 min. WRMSL data are shown in Figure F7. After the 14 h repose, one interval of low bulk density had increased in density by more than 10%, and overall, there is slightly less variability in density along the section. There is no change in MS, however. During the 14 h interval, the section was stored horizontally and subjected only to the gentle rolling motion of the ship in calm weather and careful

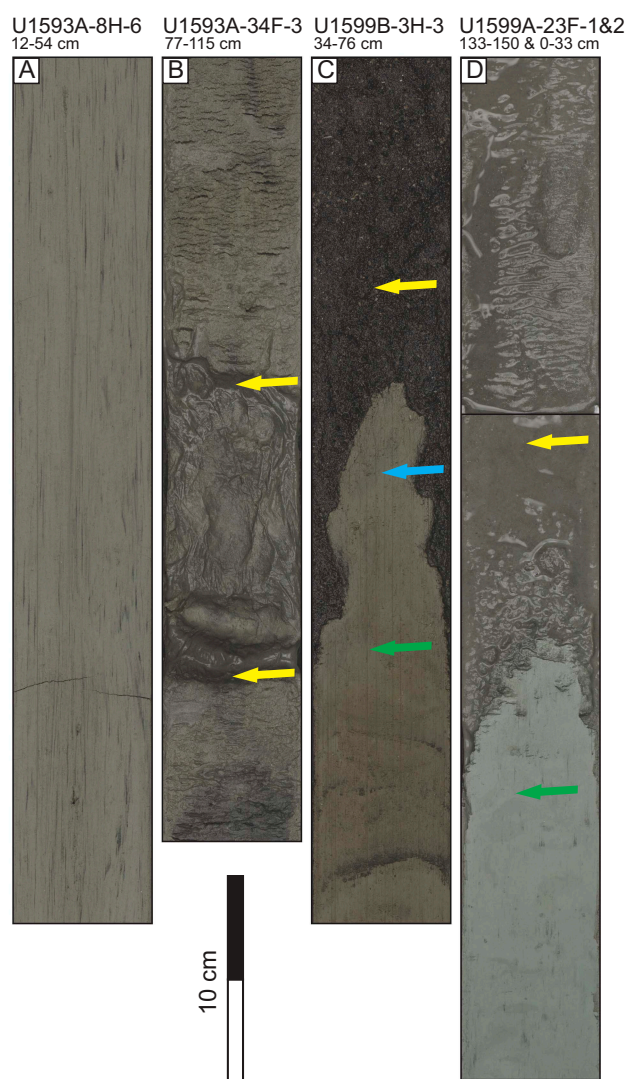


Figure F6. Examples of extension, liquefaction, and shearing, Sites U1593, U1595, and U1599. A. Black-spotted carbonate ooze intensely sheared parallel to the margins of the core liner. Compare and contrast with striated surface texture caused by scraping coarse ash across surface of muddy core during wireline cutting in C. B. Extension and liquefaction of a fine ash interval (bottom and top yellow arrows) interbedded with carbonate ooze. C, D. Sheared (blue arrow) and undisturbed (green arrow) carbonate ooze with liquefaction and loss of stratification in volcanic ash (yellow arrows). D shows standing water on top of the volcanic ash, which results from sediment dewatering.

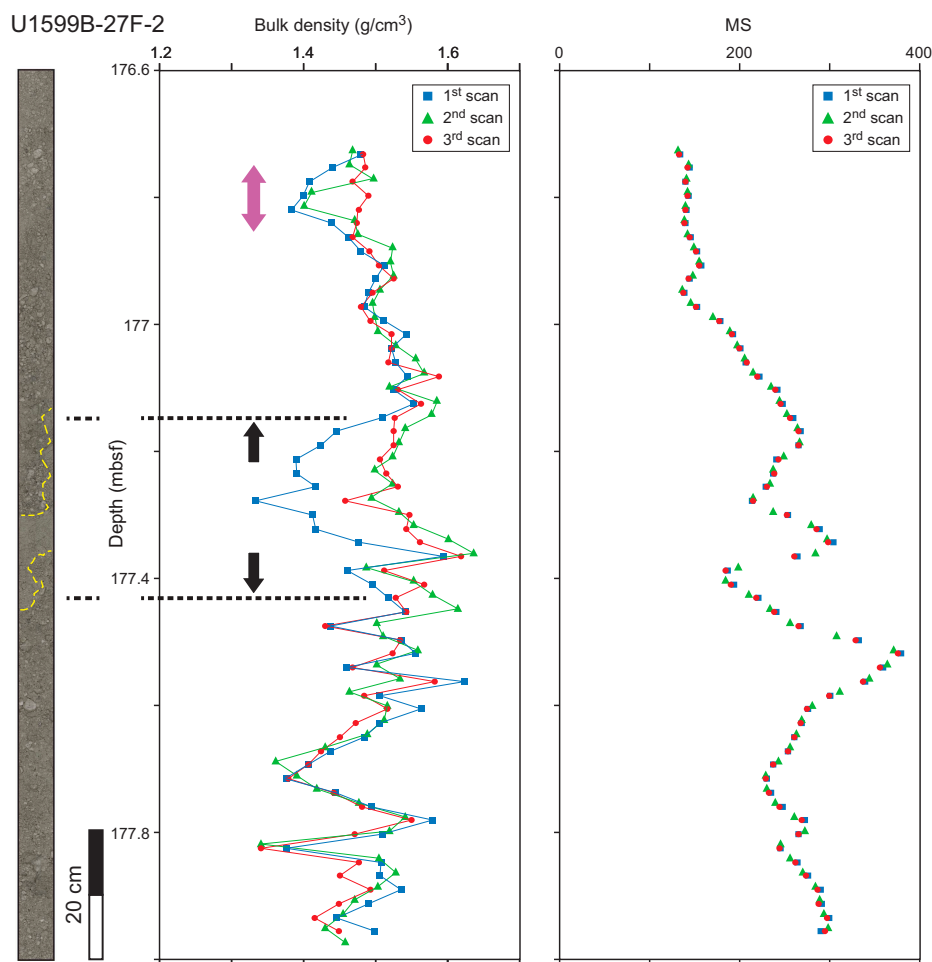


Figure F7. Bulk density and MS whole-round measurements showing on-deck disturbance (398-U1599B-27F-2). As an experiment, this section was measured 10 min after sectioning on the catwalk (first scan) and then twice more (second and third scans) after being stored horizontally onboard for 14 h. Second and third scans were separated by 9 min. Image shows archive half of same section after subsequent splitting and drying of excess water. Yellow dashed lines = ash-rich area probably generated by gentle lateral movement of fine particles during horizontal storage, matching the anomalies in the physical properties; black arrows and dashed lines = interval of significant mass redistribution between initial measurement and subsequent scans; purple arrow = smaller interval where mass redistribution only occurs between the second and third scans.

transport from the core rack to the instruments by shipboard scientists. We posit that the magnetic signal is controlled by minerals contained within pumice lapilli, which were too large to be easily redistributed laterally; meanwhile, fine-grained ash (vesicular glass) particles of lower MS and higher bulk density than lapilli were able to migrate laterally through the framework of larger clasts as the section was repeatedly tilted or handled while the core was transported between instruments and the storage rack, thus altering the along-section variation in bulk density but not MS. The split core photograph shows an ash-rich layer that might have preferentially accumulated in a specific area of the core section during storage, possibly by surficial accumulation of fines. This experiment highlights that, in addition to typical coring disturbance, physical properties of unconsolidated volcanoclastic material can also potentially be altered aboard the ship by wave motion and/or during core handling prior to measurement, particularly when sediments are liquefied.

4. Summary

Expedition 398 drilled and cored through unconsolidated volcanoclastic intervals surrounding subaerial and submarine volcanoes in the Hellenic arc, Greece. Volcanic environments are challenging to successfully drill and core, and coring disturbances can commonly affect the integrity of

the cores (Jutzeler et al., 2014, 2016). Our review of core photographs on APC cores shows that during Expedition 398, coring disturbances affected a large number of intervals, particularly where the units are very thick, coarse grained, and/or rich in pumice clasts. As described by Jutzeler et al. (2014, 2016), the technical difficulties involved with coring lapilli and coarse ash led to multiple instances of partial strokes, favoring basal flow-in coring disturbances in thick intervals that are not bound by carbonate ooze. We report fall-in, basal flow-in, and midcore flow-in, as well as lesser disturbances such as liquefaction, extension, and shearing, in addition to on-deck sediment remobilization. This report lists coring disturbances for the entirety of the APC cores collected during Expedition 398 and was produced as support to current and future researchers to avoid misinterpretation of these challenging textures and associated physical property data sets.

The coring disturbances identified in these units match those in other marine volcanic environments (Jutzeler and White, 2013; Jutzeler et al., 2014, 2016; Tamura et al., 2015), although the extent of disturbances in Expedition 398 cores is larger, probably owing to the abundance of extremely thick and coarse-grained volcanic units.

5. Acknowledgments

This research used samples and/or data provided by the International Ocean Discovery Program (IODP). We thank the crew, staff, and technicians on the research vessel (R/V) *JOIDES Resolution* during Expedition 398. We acknowledge travel support for an Australian scientist (A.S. Clark) by the Australian and New Zealand International Scientific Drilling Consortium (ANZIC); US scientists (including M. Manga) by the US Science Support Program (USSSP); Japanese scientists (including I. McIntosh) by the Japan Drilling Earth Science Consortium (J-DESC); as well as European scientists (including T. Druitt and S. Kutterolf) by IODP-France, IODP-Germany, the European Consortium for Ocean Research Drilling (ECORD), and the Université Clermont Auvergne (UCA) in France. Funding for this research was provided by the Australian Research Council Linkage Infrastructure, Equipment and Facilities (ARC LIEF; LE230100044). M. Jutzeler and A.S. Clark were funded through ANZIC research grant PCAF01X398_AClark. M. Manga was supported by a USSSP postexpedition activity (PEA) grant. We gratefully acknowledge Kathleen Marsaglia for her constructive review of the manuscript and Leah LeVay for her editorial handling.

References

- Druitt, T.H., Kutterolf, S., Ronge, T.A., and the Expedition 398 Scientists, 2024a. Hellenic Arc Volcanic Field. *Proceedings of the International Ocean Discovery Program, 398*: College Station, TX (International Ocean Discovery Program). <https://doi.org/10.14379/iodp.proc.398.2024>
- Druitt, T., Kutterolf, S., Ronge, T.A., Hübscher, C., Nomikou, P., Preine, J., Gertisser, R., Karstens, J., Keller, J., Koukousioura, O., Manga, M., Metcalfe, A., McCanta, M., McIntosh, I., Pank, K., Woodhouse, A., Beethe, S., Berthod, C., Chiyonobu, S., Chen, H., Clark, A., DeBari, S., Johnston, R., Peccia, A., Yamamoto, Y., Bernard, A., Perez, T.F., Jones, C., Joshi, K.B., Kletetschka, G., Li, X., Morris, A., Polymenakou, P., Tominaga, M., Papanikolaou, D., Wang, K.-L., and Lee, H.-Y., 2024b. Giant offshore pumice deposit records a shallow submarine explosive eruption of ancestral Santorini. *Communications Earth & Environment*, 5(1):24. <https://doi.org/10.1038/s43247-023-01171-z>
- Expedition 340 Scientists, 2013. Expedition 340 summary. In Le Friant, A., Ishizuka, O., Stronck, N.A., and the Expedition 340 Scientists, *Proceedings of the Integrated Ocean Drilling Program. 340*: Tokyo (Integrated Ocean Drilling Program Management International, Inc.). <https://doi.org/10.2204/iodp.proc.340.101.2013>
- Jutzeler, M., Clark, A.S., Manga, M., McIntosh, I., Druitt, T., Kutterolf, S., and Ronge, T.A., 2025. Supplementary material, <https://doi.org/10.14379/iodp.proc.398.203supp.2025>. In Jutzeler, M., Clark, A.S., Manga, M., McIntosh, I., Druitt, T., Kutterolf, S., and Ronge, T.A., Data report: coring disturbances in advanced piston cores from IODP Expedition 398, Hellenic Arc Volcanic Field. In Druitt, T.H., Kutterolf, S., Ronge, T.A., and the Expedition 398 Scientists, *Hellenic Arc Volcanic Field. Proceedings of the International Ocean Discovery Program, 398*: College Station, TX (International Ocean Discovery Program).
- Jutzeler, M., Talling, P.J., White, J.D.L., and the Expedition 340 Scientists, 2016. Data report: coring disturbances in IODP Expedition 340, a detailed list of intervals with fall-in and flow-in. In Le Friant, A., Ishizuka, O., Stronck, N.A., and the Expedition 340 Scientists, *Proceedings of the Integrated Ocean Drilling Program. 340*: Tokyo (Integrated Ocean Drilling Program Management International, Inc.). <https://doi.org/10.2204/iodp.proc.340.206.2016>

- Jutzeler, M., and White, J.D.L., 2013. New insights from pumice-rich submarine density currents from caldera-forming eruptions in the Izu Bonin arc (ODP 126). Presented at the IAVCEI General Assembly, Kagoshima, Japan. <https://gbank.gsj.jp/ld/resource/geolis/201324957>
- Jutzeler, M., White, J.D.L., Talling, P.J., McCanta, M., Morgan, S., Le Friant, A., and Ishizuka, O., 2014. Coring disturbances in IODP piston cores with implications for offshore record of volcanic events and the Missoula megafloods. *Geochemistry, Geophysics, Geosystems*, 15(9):3572–3590. <https://doi.org/10.1002/2014GC005447>
- Kutterolf, S., Druitt, T.H., Ronge, T.A., Beethe, S., Bernard, A., Berthod, C., Chen, H., Chiyonobu, S., Clark, A., DeBari, S., Fernandez Perez, T.I., Gertisser, R., Hübscher, C., Johnston, R.M., Jones, C., Joshi, K.B., Kletetschka, G., Koukousioura, O., Li, X., Manga, M., McCanta, M., McIntosh, I., Morris, A., Nomikou, P., Pank, K., Peccia, A., Polymenakou, P.N., Preine, J., Tominaga, M., Woodhouse, A., and Yamamoto, Y., 2024. Expedition 398 methods. In Druitt, T.H., Kutterolf, S., Ronge, T.A., and the Expedition 398 Scientists, Hellenic Arc Volcanic Field. *Proceedings of the International Ocean Discovery Program*, 398: College Station, TX (International Ocean Discovery Program). <https://doi.org/10.14379/iodp.proc.398.102.2024>
- Le Friant, A., Ishizuka, O., Boudon, G., Palmer, M.R., Talling, P.J., Villemant, B., Adachi, T., Aljhdali, M., Breitzkreuz, C., Brunet, M., Caron, B., Coussens, M., Deplus, C., Endo, D., Feuillet, N., Fraas, A.J., Fujinawa, A., Hart, M.B., Hatfield, R.G., Hornbach, M., Jutzeler, M., Kataoka, K.S., Komorowski, J.C., Lebas, E., Lafuerza, S., Maeno, F., Manga, M., Martínez-Colón, M., McCanta, M., Morgan, S., Saito, T., Slagle, A., Sparks, S., Stinton, A., Stroncik, N., Subramanyam, K.S.V., Tamura, Y., Trofimovs, J., Voight, B., Wall-Palmer, D., Wang, F., and Watt, S.F.L., 2015. Submarine record of volcanic island construction and collapse in the Lesser Antilles arc: first scientific drilling of submarine volcanic island landslides by IODP Expedition 340. *Geochemistry, Geophysics, Geosystems*, 16(2):420–442. <https://doi.org/10.1002/2014GC005652>
- McCoy, F.W., 1985. Mid-core flow-in; implications for stretched stratigraphic sections in piston cores. *Journal of Sedimentary Research*, 55(4):608–610. <https://doi.org/10.1306/212F8774-2B24-11D7-8648000102C1865D>
- Tamura, Y., Busby, C.J., Blum, P., Guèrin, G., Andrews, G.D.M., Barker, A.K., Berger, J.L.R., Bongiolo, E.M., Bordiga, M., DeBari, S.M., Gill, J.B., Hamelin, C., Jia, J., John, E.H., Jonas, A.-S., Jutzeler, M., Kars, M.A.C., Kita, Z.A., Konrad, K., Mahony, S.H., Martini, M., Miyazaki, T., Musgrave, R.J., Nascimento, D.B., Nichols, A.R.L., Ribeiro, J.M., Sato, T., Schindlbeck, J.C., Schmitt, A.K., Straub, S.M., Vautravers, M.J., and Yang, Y., 2015. Site U1436. In Tamura, Y., Busby, C.J., Blum, P., and the Expedition 350 Scientists, Izu-Bonin-Mariana Rear Arc. *Proceedings of the International Ocean Discovery Program*, 350: College Station, TX (International Ocean Discovery Program). <https://doi.org/10.14379/iodp.proc.350.103.2015>
- Taylor, B., Fujioka, K., et al., 1990. *Proceedings of the Ocean Drilling Program, Initial Reports*, 126: College Station, TX (Ocean Drilling Program). <https://doi.org/10.2973/odp.proc.ir.126.1990>